

## Optimum time history analysis of SDOF structures using free scale of Haar wavelet

S.H. Mahdavi<sup>\*1</sup> and S. Shojaee<sup>2a</sup>

<sup>1</sup>Department of Civil Engineering, Islamic Azad University, Kerman Branch, Kerman, Iran  
<sup>2</sup>Department of Civil Engineering, Bahonar University of Kerman, Kerman, Iran

(Received July 8, 2012, Revised October 25, 2012, Accepted December 1, 2012)

**Abstract.** In the recent decade, practical of wavelet technique is being utilized in various domain of science. Particularly, engineers are interested to the wavelet solution method in the time series analysis. Fundamentally, seismic responses of structures against time history loading such as an earthquake, illustrates optimum capability of systems. In this paper, a procedure using particularly discrete Haar wavelet basis functions is introduced, to solve dynamic equation of motion. In the proposed approach, a straightforward formulation in a fluent manner is derived from the approximation of the displacements. For this purpose, Haar operational matrix is derived and applied in the dynamic analysis. It's free-scaled matrix converts differential equation of motion to the algebraic equations. It is shown that accuracy of dynamic responses relies on, access of load in the first step, before piecewise analysis added to the technique of equation solver in the last step for large scale of wavelet. To demonstrate the effectiveness of this scheme, improved formulations are extended to the linear and nonlinear structural dynamic analysis. The validity and effectiveness of the developed method is verified with three examples. The results were compared with those from the numerical methods such as Duhamel integration, Runge-Kutta and Wilson- $\theta$  method.

**Keywords:** dynamic analysis; numerical approximation; Haar wavelet; operational matrix

---

### 1. Introduction

Haar basis function as a rectangular pulse pair was presented with Alfred Haar in 1910 (Fig. 1). Although in 1980s it was derived that the Haar function is the first order of Daubechies Wavelet; it seems that Haar basis is the simple basis for wavelet analysis in numerical problems (Frag 1992, Goedecker and Ivanov 1998).

Fig.1 shows that the Haar wavelet is not continuous in the point of 0.5 and at the point of discontinuity the derivatives do not exist. Hence, it is impossible to use this wavelet directly to solve high-ordered differential equations; Although, Lepik (2009) and Yuanlu Li (2010) has been presented practical of this discrete wavelet to solve several fractional differential equations. Moreover, efficiency of Haar wavelet method has been demonstrated by Lepik (2008) to solve

---

\*Corresponding author, PhD, Candidate, E-mail: [s.h.mahdavi@gmail.com](mailto:s.h.mahdavi@gmail.com)

<sup>a</sup>Assistant Professor, E-mail: [saeed.shojaee@mail.uk.ac.ir](mailto:saeed.shojaee@mail.uk.ac.ir)

higher order differential equations. In addition, initial and boundary value problems were evaluated in the case of linear or nonlinear equations by Lepik (2008).

In general, there are two possibilities to overcome the essential shortcoming of discrete Haar wavelet. First, the piecewise constant Haar functions can be regularized with interpolation splines. This method that has been applied by Cattani (2004), greatly complicates the solution. Second convenient solution, to use this wavelet is, utilizing the integral method, which the highest derivative objections in the differential equation is expanded into the Haar series. This approximation is integrated while the boundary conditions are incorporated by using integration constants. This approach has been considered for the Haar wavelet by Chen and Hsiao (1997) and an optimal control problem with the quadratic performance index was discussed by them (Cattani 2004).

In addition, Haar discrete wavelet transforms have been utilized by Cattani (2004) to achieve three goals: first, to filter the data without removing localized effective changes which is capable in the case of structural engineering to shorten components of complicated loadings such as earthquake to achieve an optimum structural dynamic scheme. Second, to classify the detected jumps and finally, to obtain a smooth trend to represent the time series evolution.

According to the technique of Chen and Hsiao (*CHM*), either linear differential equation or nonlinear one is converted into an algebraic equation. Although, in the entire time history analysis of structures, durations of intervals are important to gain the stable responses, in this method, particularly for complicated loads such as equation of motion, a long step with many collocation points makes the accurate coefficient matrix to achieve a desirable response as quick as common numerical methods, do accurately. This method that divides intervals to many points as collocation point is called segmentation method (*SM*) (Hubbard 1997, Lepik 2004).

Obviously, for smooth loadings, such as harmonic loadings, to reduce computational complexity and computation time of analysis, the interval of integration needs to be divided into fewer points (Salajeghe and Heidari 2004); this method is called reduced Haar transform (Galli *et al.* 1996). Meanwhile, in the reduced Haar transform technique the number of collocation points in each segment is smaller than in the *CHM* method is. Consequently, for some specific and simple loadings, further simplification of the solution can be obtained as long as a segment is being divided into only one node. It is assumed that the highest derivative is constant in each segment. This method is called piecewise constant approximation (*PCA*) (Chen and Hsiao 1997).

The main aim of this paper is, formulate a developed method with the free scale of Haar wavelet to optimum time history analysis of equation of motion elaborately. Moreover, results which are calculated with some numerical methods such as *CHM*, *SM* and *PCA* against various loadings with Haar wavelet have been compared with common numerical techniques. To consider efficiency of developed method, it is exemplified with a *SDOF* structure in the linear and nonlinear way. Finally, computation time involved and errors have been investigated comparatively through the proposed method and common numerical methods.

## 2. Haar wavelet basis

The family of Haar wavelet for  $t \in [0, 1]$  is defined as follow

$$H_{m-1}(t) = \begin{cases} 1 & t \in \left[ \frac{k}{2^j}, \frac{k+0.5}{2^j} \right] \\ -1 & t \in \left[ \frac{k+0.5}{2^j}, \frac{k+1}{2^j} \right] \\ 0 & \text{otherwise} \end{cases} \quad (1)$$

Where

$$m = 2^j + k + 1, \quad j \geq 0, \quad 0 \leq k \leq 2^j - 1 \quad (2)$$

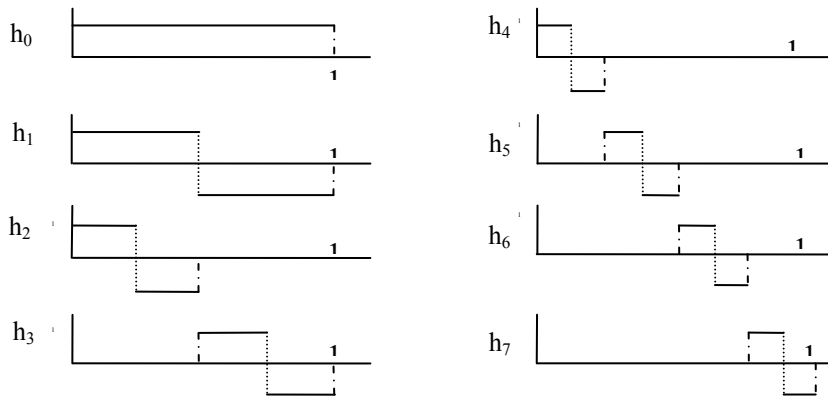


Fig. 1 Haar wavelet family (the first 8 transition of scaled wavelet)

In this formulation  $M = 2^j (j = 0, 1, \dots, j)$  indicates the order of wavelet;  $k = 0, 1, \dots, M - 1$  is the parameter of transition. To expansion of the *CHM* to the *SM* method with collocation points,  $2M$  is the number of points in segmentations that indicates the scale of Haar wavelet (Chen and Hsiao 1997). In addition, accuracy of analysis regarding to the steps and scale of wavelet depend on the number of points that are calculated in each step. Obviously, to gain the accurate responses, further points are needed in each segmentation. It means further analyzing with transition of scaled functions in each step achieves the accurate responses, although it takes a long computation time (Chen and Hsiao 1997).

Through to this method, points are increased in each computation steps in the power of  $2(2^j)$ ;  $= 1$  denotes scale function ( $h_0$  in the Fig. 1) and  $m = 2$  denotes mother wavelet of Haar ( $h_1$  in the Fig. 1). Orthogonality of Haar wavelets as obtained in Eq. (3) motivates them as one useful transition basis function for wavelet analysis in the engineering problems.

$$\int_0^1 h_i(t)h_p(t)dt = 2^{-j} \delta_{ip} = \begin{cases} 2^{-j} & i = p = 2^j + k \\ 0 & i \neq p \end{cases} \quad (3)$$

### 3. Algebraic approximation of equations with Haar wavelet

As can be seen from Fig. 1, Haar wavelet functions are expanded for 8 points as following

$$M = 2^j, \quad j = 0, 1, \dots, j = 4 \quad (4)$$

Where

$$j = 2 \rightarrow 2M = 8, \quad k = 0, 1, \dots, m - 1 \quad (5)$$

Relevantly, each function such as  $signal(t)$  expressed as

$$signal(t) = \sum_{i=0}^{2M} \omega_i h_i(t) \quad (6)$$

Thereby, Haar weight coefficients  $\omega_i$  are calculated directly as

$$\omega_i = 2^j \times \int_0^{2M} signal(t) h_i(t) dt \quad (7)$$

Through the algebraic approximation of functions, square matrixes of coefficient  $H_{2M \times 2M}$  and operation of integration  $P_{2M \times 2M}$  are improved in the following equations. In the  $H$  matrix, (Fig. 2) it is a declined trend for scale of Haar wavelet from the first row to the  $2M$ th row and shifted transition from the first column to the  $2M$ th one.

$$H_{2M} = \begin{bmatrix} \mathbf{1} & \mathbf{1} & \dots & \mathbf{A} & \dots & \mathbf{1} & \vdots & \mathbf{1} & \mathbf{1} & \dots & \mathbf{1} \\ \mathbf{1} & \mathbf{1} & \dots & \mathbf{B}_1 & \dots & \mathbf{1} & \vdots & \mathbf{-1} & \mathbf{-1} & \dots & \mathbf{-1} \\ & & & \vdots & \nearrow & & \vdots & \searrow & & \vdots & \\ & & & \vdots & \nearrow & & \mathbf{B}_2 & & & \vdots & \\ \mathbf{1} & \mathbf{1} & \mathbf{-1} & \mathbf{-1} & \mathbf{0} & & \mathbf{0} & \mathbf{0} & \mathbf{0} & \dots & \mathbf{0} \\ \mathbf{0} & \mathbf{0} & \mathbf{0} & & & & \dots & \dots & \mathbf{1} & \mathbf{1} & \mathbf{-1} & \mathbf{-1} \\ \mathbf{1} & \mathbf{-1} & \mathbf{0} & \mathbf{0} & \mathbf{0} & & & & & \dots & \mathbf{0} \\ & & & & \searrow & \mathbf{B}_{2M} & \searrow & & & & & \end{bmatrix}$$

Fig. 2 Schematic format of Haar wavelet coefficients matrix in the SM method

Where the block  $A$  is the scale block,  $B_j$  is the Haar mother wavelet, and from the first block to the end, the scale of Haar wavelet is declined. This numerically developed matrix shows that from a column to next one the scaled wavelet has been shifted to make an elaborate algebraic system. Thereby, dimension of  $B$  blocks from  $B_{2M}$  to  $B_1$  follows the rule of

$$B(2M/2^i, 2M) \rightarrow (i = 1, 2, \dots, j + 1), A(1, 2M) \quad (8)$$

Where

$$2^i = 1, 2, \dots, j + 1 \quad (9)$$

For instance, if  $2M = 8$ ,  $H$  matrix is developed as

$$H_8 = \begin{bmatrix} 1 & 1 & 1 & 1 & 1 & 1 & 1 & 1 \\ 1 & 1 & 1 & 1 & -1 & -1 & -1 & -1 \\ 1 & 1 & -1 & -1 & 0 & 0 & 0 & 0 \\ 0 & 0 & 0 & 0 & 1 & 1 & -1 & -1 \\ 1 & -1 & 0 & 0 & 0 & 0 & 0 & 0 \\ 0 & 0 & 1 & -1 & 0 & 0 & 0 & 0 \\ 0 & 0 & 0 & 0 & 1 & -1 & 0 & 0 \\ 0 & 0 & 0 & 0 & 0 & 0 & 1 & -1 \end{bmatrix} \quad (10)$$

In addition of direct way, weight function of  $\omega_i$  is indirectly calculated via functions' matrix of loading, multiplied by inverse of coefficient matrix of Haar wavelet ( $H_{2M}^{-1}$ )

$$\omega_i = \text{signal}(t) \times H_{2M}^{-1} \quad (11)$$

Next, operation of integration matrix  $P_{2M \times 2M}$  is defined by the following equation

$$\int_0^J H_{2M}(t) dt = PH_{2M}(t) \quad (12)$$

However, Chen and Hsiao presented an equation for this square matrix, for simplifying this equation in computer programming in a sequenced way, it is developed tersely as

$$P_{2M} = \begin{bmatrix} P_M & \frac{-H_M}{4M} \\ \frac{H_M^{-1}}{4M} & 0 \end{bmatrix} \quad (13)$$

#### 4. Solution of the second-ordered differential equations via Haar wavelet

According to the collocation method, after dividing time dependent lateral force to the  $N$  equal segmentations with length of  $d_n$ , local nodes are defined. For example, it is considered as  $SM 4$  as long as intervals are divided to the 4 points. Thereby, local points are introduced as

$$\tau_j = \frac{1}{2M}(j - 0.5), \quad J = 1, 2, \dots, 2M \quad (14)$$

Next, to convert local time to the global computation time ( $t_j$ )

$$t_{jn} = d_n(\tau_j) + t_n \rightarrow \tau_j = \frac{t_n - t_{jn}}{d_n}, \quad (j = 1, 2, \dots, 2M) \quad (15)$$

To approximate the following ODE

$$\frac{d^2 u}{dt^2} = F\left(t, u, \frac{du}{dt}\right), \quad t \in (0, t) \quad (16)$$

The first order of equations is used, instead

$$\frac{du}{dt} = v \quad (17)$$

$$\frac{dv}{dt} = \frac{d^2 u}{dt^2} = F(t, u, v) \quad (18)$$

To convert new equations to the local time, these are considered by

$$\frac{du}{d\tau} = v \cdot d_n \quad (19)$$

$$\frac{dv}{dt} = d_n \cdot F(t_n + d_n(\tau_j), u, v) \quad (20)$$

$u, v$  are row vectors as

$$u_j = u(\tau_j), \quad v_j = v(\tau_j), \quad j = 1, 2, \dots, 2M \quad (21)$$

For instance in *SM 4* the vector of velocity and displacement are defined as

$$\bar{u} = [u_1 \ u_2 \ u_3 \ u_4], \quad \bar{v} = [v_1 \ v_2 \ v_3 \ v_4] \quad (22)$$

For algebraic expansion of the first derivation, via Haar wavelet in *PCA* method it is considered as

$$\dot{u} = a H(t) \rightarrow u = \int_0^t \dot{u}(\tau) d(\tau) + u_0 = \int_0^t a H(\tau) d(\tau) + u_0 = a PH(t) + u_0 \quad (23)$$

Equivalently, velocity is simplified as

$$\dot{v} = b h(t) \rightarrow v = b PH(t) + v_0 \quad (24)$$

Next, it is defined as an algebraic system in *SM<sub>2M</sub>* method

$$\begin{cases} \dot{v} = b H, & v = b PH + v_n E \\ \dot{u} = a H, & u = a PH + u_n E \end{cases} \quad (25)$$

Here  $a, b$  are row vectors with dimension of  $2M$ , for multiplying with  $aPH$  or  $bPH$  an unit vector is suffixed as  $E_{1 \times 2M}$ . Finally  $u_n, v_n$  are initial and boundary conditions in  $t = t_n$ , that are obtained with linear interpolation of  $u_1$  in the current interval and  $u_{2M}$  is derived from previous interval. Substitution of Eq. (22) into Eq. (23) gives

$$aH = d_n(b PH + v_n E), \quad bH = d_n F(t_n + d_n \tau, aH + u_n E, b PH + v_n E) \quad (26)$$

Consequently, this algebraic system is solved and gives  $a, b$ . After considering about initial conditions, velocity and acceleration are obtained as

$$u_{n+1} = a_1 + u_n E \quad (27)$$

$$u_{n+1} = b_1 + v_n E \quad (28)$$

Here  $a_1, b_1$  are the first components of vector  $a$  and  $b$  in each step (Lepik 2004).

## 5. Solution of dynamic equation of motion via free scale of Haar wavelet

The second ordered *ODE* for the dynamic equilibrium in the global time is considered as

$$m \frac{d^2 u}{dt^2} + c \frac{du}{dt} + k \cdot u = f_0 \cdot f(t) \quad (29)$$

Where in the linear behaviors, stiffness ( $K$ ) and damping ( $C$ ) and mass ( $m$ ) are constants. After discretization of external loading  $f_0 \cdot f(t)$  to the  $N$  equal intervals,  $2M$  points are considered in each  $d_n$  as collocation points and finally it is converted to the local time analysis as follow

$$\frac{d^2 u}{dt^2} + \frac{c}{m \cdot d_n} \cdot \frac{du}{dt} + \frac{k}{m \cdot d_n} \cdot u = \frac{f_0}{m \cdot d_n} \cdot f(t_n + d_n \tau) \quad (30)$$

Where, term of velocity and acceleration are considered as

$$\dot{u} = d_n \cdot v \quad (31)$$

$$\dot{v} = -\frac{c}{m d_n} \cdot v - \frac{k}{m d_n} \cdot u + \frac{f_0}{m d_n} \cdot f(t_n + d_n \tau) \quad (32)$$

Or equivalently are expanded as

$$v = b PH + v_n E = aH \quad (33)$$

$$\dot{u} = d_n b PH + d_n v_n E = aH \quad (34)$$

With assumption of  $= EH^{-1}$ , it gives vector of  $a_{1 \times 2M}$  as

$$a = d_n bP + d_n v_n Y \quad (35)$$

Where

$$E = [1, 1, \dots, 1]_{1, 2M} \quad (36)$$

Substitution of Eq. (32) into Eqs. (23), (29), vector of  $b_{1 \times 2M}$  is developed as

$$b_{1, 2M} = \left[ -\left( \frac{k \cdot d_n^2 \cdot v_n \cdot Y \cdot P}{m} \right) - \left( \frac{c \cdot d_n \cdot v_n + k \cdot d_n \cdot v_n}{m} \right) \cdot Y + \frac{f_0 \cdot f(t_n + d_n \tau) \cdot d_n \cdot H^{-1}}{m} \right] \times \dots \\ \dots \left[ \frac{k \cdot d_n^2 \cdot P^2}{m} + I + \frac{c \cdot d_n \cdot P}{m} \right]^{-1} \quad (37)$$

Here  $I$  stands for the  $2M$  dimensional identity matrix and function of load in the local time is defined with a vector matrix as

$$F(t_n + d_n\tau) = [\dots]_{I \times 2M} \quad (38)$$

Finally, with substituting Eqs. (32), (34) into Eqs. (25), (26) vectors of acceleration and velocity in each collocation point will be calculated. However, this procedure illustrates that for high accurate responses further points should be chosen; it takes long calculation time that is not optimized way, particularly for multi-degree of freedom structures such as continuum structures. Similarly, to extend this method in the nonlinear structures, the preceding provisions in previous step are calculated as new conditions in current step for each nonlinear behavior.

## 6. Computer program code development

To investigate elaborately about efficient and free scale of Haar wavelets a comprehensive program is codified in *MATLAB*. In addition, it has expanded for time history linear and nonlinear dynamic analysis of *SDOF* structures, through the following steps:

### Part-A: Initial calculation:

- 1-Formulate Haar wavelet coefficient matrix ( $H$ ) relevantly to the scale and transition factor due to the lateral loading and desirable accuracy of results (Fig. 2).
- 2-Formulate operation of integral ( $P$ ) matrix of Haar wavelet relevantly to the  $H$  matrix of Haar wavelet (Eq. (13)).
- 3-Formulate local time due to collocation points of scaled Haar wavelet (Eq. (15)).
- 4-Discretization of the lateral load into  $N$  equal intervals and approximate the value of loading according to the Haar polynomials (Eq. (35)) for each time step.

### Part-B: calculation in each time step:

- 1-Define a constant for the mass ( $M$ ), stiffness ( $K$ ) and damping ( $C$ ) of *SDOF* structure in each time step. For instance, in the nonlinear study this constant will be defined from the previous step according to the relation of nonlinearity.
- 2-Calculation of the initial conditions due to  $a$ ,  $b$  by solving the relevant algebraic equation systems. (Eqs. (34), (32)).
- 3-Calculation of the velocity ( $\dot{U}$ ), displacement ( $U$ ) in each step as initial condition of next step (Eqs. (25), (26)).

However, nonlinearity also can be expanded with Haar wavelet; in this study nonlinearity has been applied in each time steps by calculation of initial conditions, which are calculated from previous steps.

## 7. Numerical applications

The accuracy and computation time of diverse scale of Haar wavelet have been evaluated in comparison of responses which are computed with prevalence dynamically numerical methods through the three models.

7-1: The *SDOF* structure which concentrated harmonic loading  $F(t) = 5.\sin(2t)$  is applied to the rigid floor is considered with following members' characteristics (Fig. 3): According to the equal

frequency for lateral loading and Structure, results which are calculated from resonance formulation will be checked out ( $I = 25170 \text{ cm}^4$ ,  $E = 2.1 \times 10^6 \text{ kg/cm}^2$ ,  $k = 24 \text{ EI/L}^3$ ).

This example was analyzed by free scales of Haar wavelet and 2 methods including Duhamel method which the time increment is selected by  $dn = 0.01\text{s}$  and resonance formulation. Responses from Runge-Kutta method have been calculated as exact method and errors ( $\Delta e$ ) are presented in comparison with Runge-Kutta results. Results including the value of the displacements for shear degree of freedom have been calculated and plotted in Fig. 4.

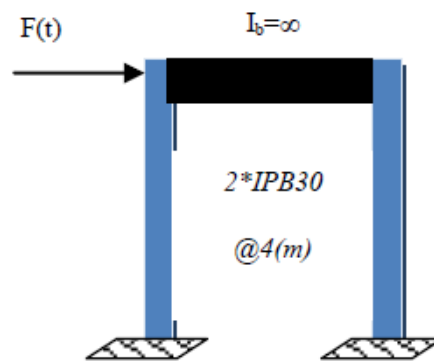


Fig. 3 SDOF model

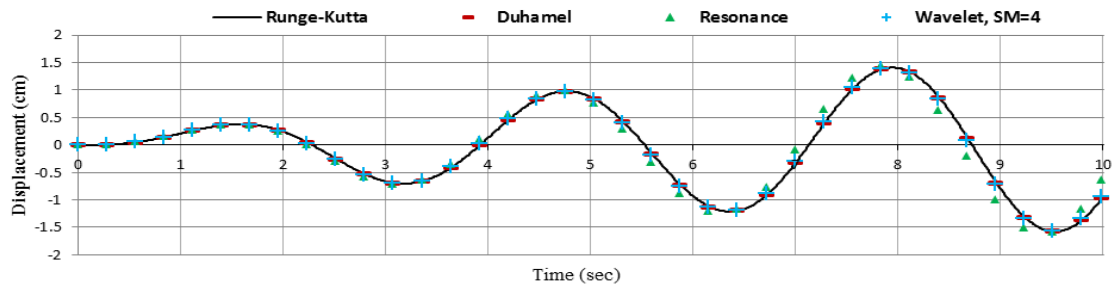


Fig. 4 Comparison of linear system for harmonic loading (Ex. 1)

Table 1 Absolute error and calculation time of model 7-1 with free scale of Haar wavelet

Haar Wavelet, 10 sec loading, $dn = 0.01$								
	PCA	SM2	SM4	SM8	SM16	SM32	SM64	SM128
$t$ (sec)	1.4894	2.0628	2.7254	4.5271	7.3592	13.8257	27.6564	64.5791
$\Delta e$	7.60E-04	6.00E-04	5.90E-04	9.20E-05	8.00E-05	6.30E-05	5.00E-05	5.00E-05

Table 2 Absolute error and computation time of exact and prevalence methods for model 7-1

Time of loading (T)=1 sec, $dn = 0.01$	$t$ (sec)	$\Delta e$
Duhamel with damping	1.4578	4.00E-05
Resonance equation with damping	1.4395	3.35E-02
Exact Runge-Kutta method	47.0795	-

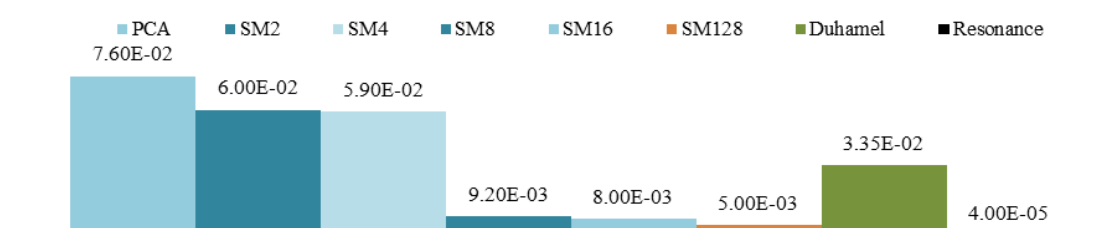


Fig. 5 Average errors in displacement of SDOF based on diverse scale of Haar wavelet (Ex. 7-1)

In addition, computational time and exact error of responses for each method have been shown in Tables 1 and 2. Table 1 shows that, albeit computation time in the *PCA* reaches to the minimum amount of 1.49 sec, but value of error with  $7.6E-04$  in comparison with other scales makes undesirable responses. Finally, percentages of errors have been calculated separately for various scaled and translated Haar wavelet, Duhamel and resonance formulation (Fig. 5).

It can be seen overtly from Fig. 5 that errors have a downward trend in the first 3 scale of Haar wavelet. Despite the fact that, Fig. 5 illustrates value of errors decreased significantly in high scale of Haar wavelet, data in Tables 1 and 2, show that computational time involved has been sharply increased due to the high scale of Haar wavelet (*SM32*, *SM64* and *SM128*). However, it was calculated that the results from high scale of Haar wavelet are closer than low ones; computational time involved for high scale of this wavelet makes suboptimal solution way. As a result, it can be evaluated comparatively from data that desirable results have been calculated with low scale of Haar wavelet in comparison with common numerical methods particularly for smooth loadings.

7-2: The *SDOF* model which was considered in model 1 (Fig. 3) is excited by Elcentro acceleration (ImperialValley-1940) as shown in Fig. 6 and the linearly dynamic analysis is carried out.

In this instance, to validate proposed method *SDOF* structure (Fig. 3) has been solved under seismic excitation as ground acceleration of Elcentro (Fig. 6). Calculated results have been compared with common direct integration method due to the Duhamel method. Duhamel's results being computed in time increment  $dn = 0.01s$ . Time history analysis of displacements are plotted in Figs. 7, 8 respectively for the first 10 and 1 second of Elcentro and calculated in Table 3 for free scale of Haar wavelet in comparison with Duhamel method.

Furthermore, average percentages of errors in compare of Duhamel are calculated in Fig. 9 and in Fig. 10 respectively computational time has been investigated for proposed method. What is

more, time history responses for displacement of SDOF are plotted for the first one second of complex lateral loading and computational time has been investigated in Table 3 for two comprehensive scales of Haar wavelet and Duhamel method.

Table 3, Fig. 9 and Fig. 10 indicate that 16<sup>th</sup> scale of Haar wavelet makes less computation time and closer responses rather than other scale of Haar wavelet. According to the Fig. 9, although fewer errors belong to the 128<sup>th</sup> scale of Haar wavelet; time consumption of this scale due to the Fig. 10 is in the maximum pick that for this complex loading will be non-optimal. Overall, time history analysis of SDOF structure under complex loading which is consist of divers frequencies, indicates that higher scale of Haar wavelet which covers various frequency of loading achieves accurate responses albeit the computational time involved has been drastically increased.

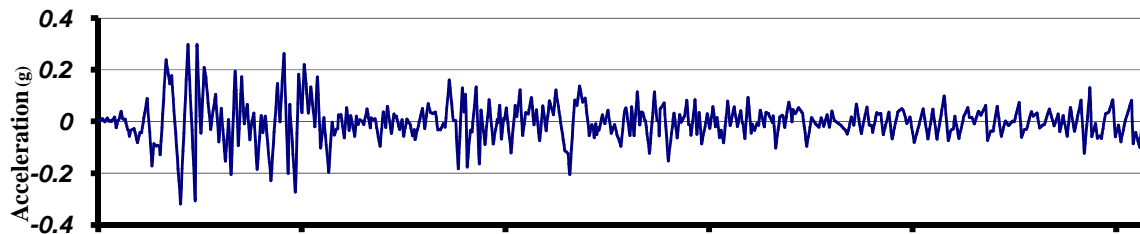


Fig. 6 Elcentro-USA (Imperial Valley-1940) earthquake acceleration record (g)

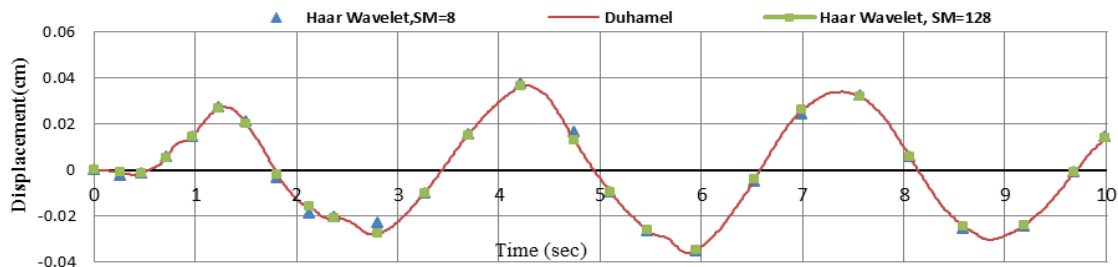


Fig. 7 Comparison of linear system for Elcentro acceleration with free scale of Haar wavelet in the first 10 seconds

Table 3 Absolute errors and computation times of Duhamel and free scale of Haar wavelet for example 7-2

	Haar Wavelet, 10 sec loading, $dn = 0.01$					Direct integration			Duhamel
	PCA	SM2	SM4	SM8	SM16	SM32	SM64	SM128	
$t$ (sec)	2.6196	3.0628	4.5788	7.3447	13.173	24.3701	48.4159	102.5703	14.1404
$\Delta e$	3.65E-02	3.53E-02	3.45E-02	2.40E-02	2.35E-02	1.30E-03	5.40E-04	6.00E-05	-

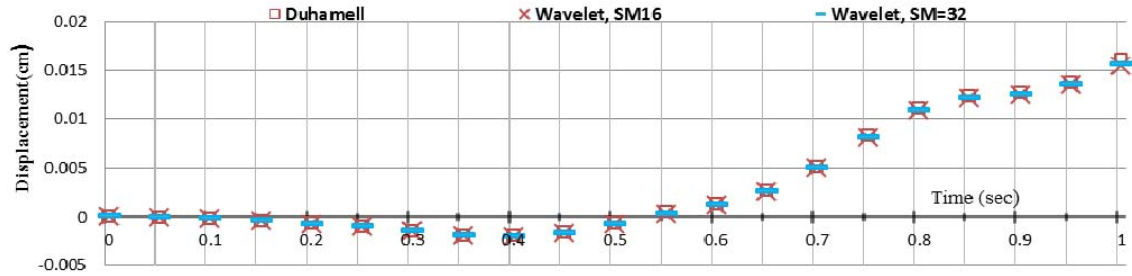


Fig. 8 Comparison of linear system for Elcentro acceleration with free scale of Haar wavelet in the first 1 second

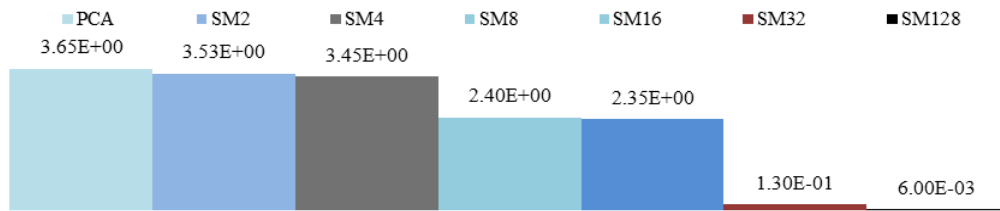


Fig. 9 Average errors in displacement of SDOF based on diverse scale of Haar wavelet (Ex. 7-2)



Fig. 10 Computational time (Sec) for diverse scaled Haar wavelet analysis (Ex. 7-2)

Table 4 Absolute error and computation time of Duhamel and two scale of Haar wavelet for example 7-2

	Haar Wavelet, 1 sec loading, $dn = 0.01$		Direct integration
	SM8	SM16	Duhamel
$t$ (sec)	1.2905	1.9375	1.4123
$\Delta e$	3.67E-02	1.90E-03	-

7-3: The *SDOF* model which was considered in model 1 (Fig. 3) is excited by Elcentro acceleration (Imperial Valley-1940) as shown in Fig. 6 and the nonlinearly dynamic analysis is carried out. For considered model the nonlinear stiffness is defined in term of displacement as

$$k = 4000 / \sqrt{abs(u) + 1} \tag{39}$$

Which  $u$  denotes initial displacement in each interval.

In this example SDOF structure Fig. 3 has been solved nonlinearly under excitation of Elcentro Fig. 6. Nonlinearity of the stiffness is defined as a function of displacement in each time step. Results which have been calculated with Wilson ( $\theta = 1.4$ ) in time increment of  $dn = 0.001s$ , are supposed as exact responses and errors ( $\Delta e$ ) are validated through the proposed method.

Time history analysis of displacement has been plotted in Figs. 11 and 12 respectively for the first 10 and 2 second of complex loading. Errors are calculated for 3 different Wilson ( $\theta = 1.4$ ) method including  $dn$  equal to 0.05, 0.1 and 0.2 s and free scale of Haar wavelet method in Fig.13.

Table 6 indicates that, computation time for simple nonlinear analysis through the Wilson method, at the first 2 seconds has been increased directly related to the duration of intervals from 1.6 to 2.9 sec.

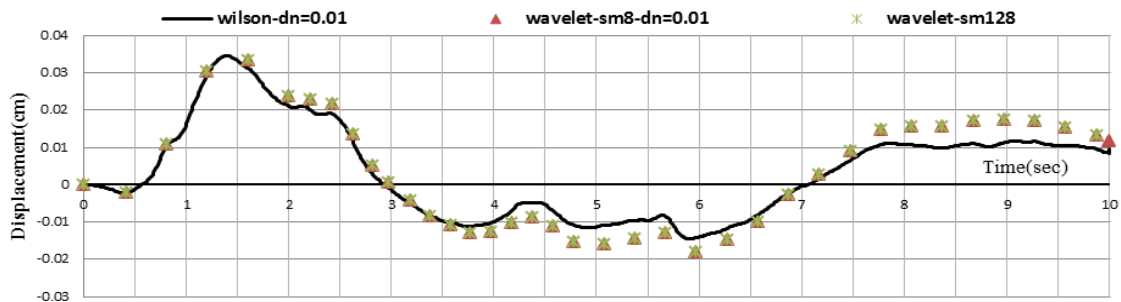


Fig. 11 Comparison of nonlinear system for Elcentro acceleration with free scale of Haar wavelet in the first 10 seconds

Table 5 Absolute error and computation time of Haar wavelet for example 7-3 in the first 2 seconds of loading

	Haar Wavelet, 2 sec loading, $dn = 0.01$							
	PCA	SM2	SM4	SM8	SM16	SM32	SM64	SM128
$t$ (sec)	1.2862	1.4221	1.6664	2.1105	2.9968	4.8411	8.7217	17.4492
$\Delta e$	3.62E-03	8.93E-04	6.30E-04	7.00E-05	5.60E-05	3.00E-05	1.90E-05	8.50E-06

Table 6 Computation time for various intervals in Wilson- $\theta$  method for example 7-3

Wilson ( $\theta = 1.4$ ), 2 sec loading	
$dn = 0.1$	1.2558
$dn = 0.01$	1.5586
$dn = 0.05$	1.3298
$dn = 0.001$	2.8933

As a result, for a complete analysis of structure at the first 20 sec against a complex loading this amount is not acceptable and makes inefficient numerical solution way. On the other hand, data which are shown at the Fig. 12 and Table 7, illustrate efficiency of proposed numerical method for the low scale of Haar wavelet for the first 2 and 10 seconds of loading.

Fig. 13 obviously shows that the first 2 scale of Haar wavelet compute inaccurate responses although with less computation time. Furthermore, it shows that it is an abrupt decline from *SM4*, *SM8* without considerable computation time involved. Consequently, in comparison with the others this scale of Haar wavelet is more accurate one with less computational time even with Wilson- $\theta$  method. Significantly, because of complex loading and complex characteristic of sample modeling it is predictable that optimum responses will be calculated approximately with proposed method.

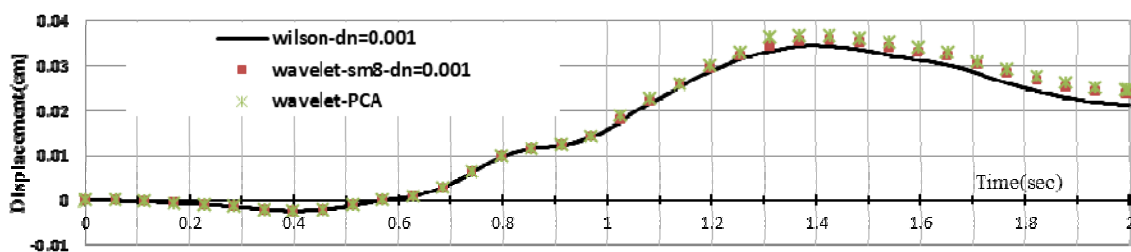


Fig. 12 Comparison of nonlinear system for Elcentro acceleration with free scale of Haar wavelet in the first 2 seconds

Table 7 Absolute error and computation time of Wilson and Haar wavelet in various intervals for example 7-3

	<i>T</i> (loading-sec)	<i>dn</i>	<i>t</i> (sec)	$\Delta e$
Wilson ( $\theta = 1.4$ )	10	0.01	1.9735	-
Haar Wavelet <i>SM4</i>	10	0.01	6.0299	8.20E-04
Wilson ( $\theta = 1.4$ )	2	0.001	3.2518	-
Haar Wavelet <i>SM32</i>	2	0.001	12.8882	9.70E-06

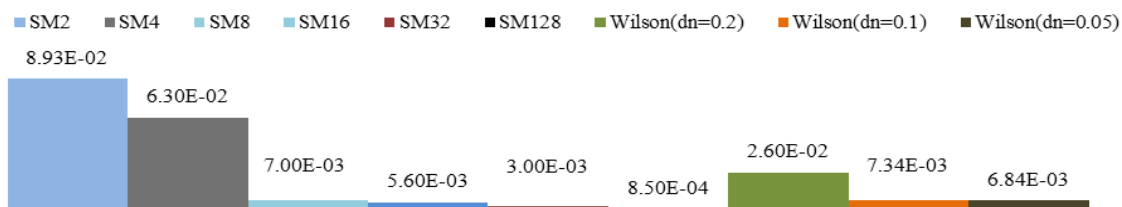


Fig. 13 Average errors in displacement of one DOF, based on diverse scale of Haar wavelet (Ex. 7-3)

## 8. Conclusions

In this paper, through the optimally dynamic analysis of structures following conclusions are carried out as:

1. Dynamic equation of motion has been analyzed coherently with accurate approximation of complex loading. Overtly, it makes distinction of this method against common numerical methods such as Duhamel or Wilson which a short interval should be chosen to gain the desirable responses. Eventually, it takes a long computational time especially for multi-degree of freedoms' structures.
2. It illustrates that the Haar wavelet is more efficient and optimum wavelet for analyzing of smooth loadings such as harmonic ones, with less collocation points.
3. Fundamentally, in one sense of analysis, combination of more collocation points in complicated steps of loading which are consist of various frequencies, and less ones in smooth steps of loading gives the optimized responses.
4. Despite accurate responses in high scale of Haar wavelet due to the inherent shape function of this wavelet, it was investigated that it is not the most optimum one in dynamic analysis of complex loading such as earthquake which are governing to the *SDOF* or *MDOF* structures.
5. Overall, according to the simple and discrete shape function of Haar wavelet an indirect way has been done for dynamic analysis. Alternatively, computation time involved has been considerably increased. Consequently, it will be suggested to try the continuous basis function in wavelet method to analyze the equation of motion directly.

## References

- Babolian, B. and Fatahzadeh, F. (2010), "Numerical solution of differential equations by using Chebyshev wavelet operational matrix of integration", *Appl. Maths. Comput.*, 188, 417-426.
- Cattani, C. (2004), "Haar wavelets based technique in evolution problems", *Proc. Estonian Acad. of Sci. Phys. Math.*, 53(1), 45-63.
- Cattani, C. (2004), "Haar wavelet based technique for sharp jump classification", *Mathematical and Computer Modeling*, 39, 255-279.
- Chen, C.F. and Hsiao, C.H. (1997), "Haar wavelet method for solving lumped and distributed-parameter system", *IEE Proc. Control Theory Appl.*, 144(1), 87-94.
- Chen, C.F. and Hsiao, C.H. (1997), "Wavelet approach to optimizing dynamic systems", *IEE Proc. Control Theory Appl.*, 16, 146.
- Chopra, A.K. (1987), *Dynamic of Structures: Theory and Applications to Earthquake Engineering*, Prentice-Hall, Englewood Cliffs, NJ.
- Frag, M. (1992), "Wavelet transforms and their application to turbulence", *Ann. Rev. Fluid Mech.*, 24, 395-457.
- Galli, A.W., Heydt, G.T. and Ribeiro, P.F. (1996), "Exploring the power of wavelet analysis", *IEEE Computer Application in Power*, 9(4), 37-41.
- Goedecker, S. and Ivanov, O. (1998), "Solution of multi scale partial differential equations using wavelets", *Comput. Phys.*, 12, 548-555.
- Hubbard, B.B. (1996), *The world according to wavelets*, Peters, A.K., Wellesley.
- Lepik, U. (2005), "Numerical solution of differential equations using Haar wavelets", *Mathematics and Computers in Simulation*, 68, 127-143.
- Lepik, U. (2008), "Haar wavelet method for solving higher order differential equations", *Int. Journal. Math. and Comput.*, 1, 84-94.

- Lepik, U. (2009), "Solving fractional integral equations by the Haar wavelet method", *Appl. Maths. Comput.*, 214, 467-481.
- Lepik, U. (2009), "Haar wavelet method for solving stiff differential equations", *Mathematical Modeling and Analysis*, 14(1), 467-481.
- Misiti, M., Misiti, Y., Oppenheim, G. and Poggi, J.M. (2001), *Wavelet toolbox user guide: for use with matlab*, Math. Works.
- Orbit, Z. and Momani, S. (2008), "Numerical method for nonlinear partial differential equations of fractional order", *Appl. Math. Modeling.*, 32, 28-39.
- Salajeghe, E. and Heidari, A. (2004), "Time history dynamic analysis of structures using filter bank and wavelet transform", *Struct. Multi-Disciplinary Opti.*, 28, 277-285.
- Yuanlu, Li. (2010), "Solving a nonlinear fractional differential equations using Chebyshev wavelet", *Commun Nonlinear Sci. Numer. Sim.*, 15, 2284-2292.